[CANCER RESEARCH 63, 4472–4480, August 1, 2003]

Rapamycin Inhibits the Interleukin 10 Signal Transduction Pathway and the Growth of Epstein Barr Virus B-cell Lymphomas[1]

Ronald R. Nepomuceno, Cynthia E. Balatoni, Yaso Natkunam, Andrew L. Snow, Sheri M. Krams, and Olivia M. Martinez[2]

Departments of Surgery, [R. R. N., C. E. B., S. M. K., O. M. M.] and Pathology, [Y. N.] and Program in Immunology, [A. L. S., S. M. K., O. M. M.], Stanford University School of Medicine, Stanford, California 94305

ABSTRACT

EBV-infected B-cell lymphomas are a potentially life-threatening complication in bone marrow and solid organ transplant recipients. Immunosuppressive drugs required to prevent allograft rejection also impair anti-EBV T-cell immunity, thereby increasing the risk of EBV-associated disease. Here we demonstrate that the immunosuppressant rapamycin (RAPA) has a strong antiproliferative effect *in vitro* on B-cell lines derived from organ transplant recipients with EBV-associated posttransplant lymphoproliferative disorder (PTLD). Furthermore, RAPA significantly inhibits or delays the growth of solid tumors established from EBV-infected B-cell lines in a xenogeneic mouse model of PTLD. RAPA acts via cell cycle arrest, induction of apoptosis, and, most importantly, inhibition of interleukin 10 secretion, a necessary autocrine growth factor. The reduced interleukin 10 production is accompanied by corresponding decreases in the constitutive activation of the growth-promoting transcription factors signal transducer and activator of transcription 1 and 3. Thus, RAPA can limit B-cell lymphoma growth while simultaneously providing immunosuppression to prevent graft rejection in patients who are otherwise at risk for EBV-associated PTLD. Moreover, these findings may have application to other EBV-associated malignancies.

INTRODUCTION

EBV is a B lymphotrophic herpesvirus associated with multiple human malignancies including nasopharyngeal carcinoma, Burkitt lymphoma, and Hodgkin's lymphoma (1, 2) EBV is also the causative agent of the B-cell lymphomas in immunocompromised and iatrogenically immunosuppressed individuals (3). Solid organ and bone marrow transplant recipients are at increased risk for EBV-related malignancies because the immunosuppressive drugs required for prevention of graft rejection also impair host anti-EBV T-cell immunity.

In healthy individuals, EBV is maintained for the lifetime of the host as an episome in a subset of resting, peripheral memory B cells that express at most two virally encoded genes, *EBNA*1 and *LMP2A* (4). The limited expression of viral antigens in infected B cells contributes to viral persistence through immune evasion. Intermittent reactivation of the virus in infected cells can give rise to activated B-cell blasts. However, the accompanying expression of the viral latent gene program is sufficient for detection and elimination by EBV-specific CTLs, thereby preventing lymphoproliferation in immunocompetent hosts.

EBV infection of B lymphocytes *in vitro* leads to immortalization and the establishment of long-term LCLs.[3] The phenotype and viral gene expression profile of LCLs recapitulates that of the lymphoblasts that arise *in vivo* during primary infection, as well as the B-cell lymphomas associated with PTLD (5). Proliferation of EBV^+ B lymphoblasts is governed by a complex interplay of viral and cellular growth and survival signals. For example, the oncogenic viral membrane protein LMP1 acts as a constitutively active, ligand-independent analogue of the B-cell surface molecule CD40 (6, 7) providing potent survival and proliferative signals.

Several lines of evidence indicate that autocrine cytokine pathways involving IL-6 and IL-10 are essential for the growth of EBV^+ B cells. Neutralizing antibodies to IL-6 inhibit *in vitro* proliferation of EBV^+ B-cell lines (8, 9) and tumor growth in SCID mice inoculated with EBV^+ B-cell lines from patients with PTLD (10) or with lymphocytes from normal, seropositive donors (11). Similarly, we and others have shown that blockade of an autocrine IL-10 loop significantly inhibits proliferation of EBV^+ B-cell lines derived from patients with PTLD (12) and AIDS-related B-cell lymphoma (13). We also showed that STAT1, STAT3, Jak1, Jak2, Jak3, and Tyk2 are constitutively tyrosine phosphorylated in EBV^+ B-cell lymphomas, consistent with autocrine IL-10 signaling (14). Constitutive activation of the Jak/STAT pathway has been associated with multiple human malignancies including EBV-related Burkitt lymphoma (15) and multiple myeloma (16) and may contribute to uncontrolled growth, oncogenic transformation, or resistance to apoptosis (17).

RAPA is a microbial macrolide with potent immunosuppressive activity and proven clinical efficacy in the prevention of organ transplant rejection (18). RAPA has also shown promise as an anticancer drug (19). In lymphoid cells, RAPA inhibits cytokine-induced proliferation and causes arrest in the G_1 phase of the cell cycle (20). RAPA interacts with the intracellular protein FK506-binding protein 12, forming a protein-drug complex that binds with high affinity to the mTOR (also known as FRAP1), a key regulatory kinase. Formation of this complex blocks mTOR function, thereby affecting multiple downstream signaling pathways required for protein synthesis and cell cycle progression.

Here we show that RAPA acts to suppress the *in vitro* and *in vivo* growth of EBV-infected B cells from patients with PTLD through a novel mechanism. RAPA inhibits production of the autocrine growth factor IL-10, thereby preventing tyrosine phosphorylation and formation of activated DNA-binding dimers of STAT1 and STAT3. In addition, RAPA induces cell cycle arrest and promotes apoptosis of EBV-infected B-cell lymphomas. Thus, RAPA is unique among the primary immunosuppressants used in clinical transplantation in that it may confer the dual advantage of preventing graft rejection while mitigating the development of EBV^+ B-cell lymphomas.

MATERIALS AND METHODS

Antibodies and Reagents. Unless otherwise specified, all reagents were obtained from Sigma (St. Louis, MO). The following antibodies were used: antihuman CD20 (clone L26) and anti-Ki-67 (clone MIB-1) mAbs (DAKO, Carpinteria, CA); rabbit antihuman STAT1α (C-24) and rabbit antihuman STAT3 [H-190 (Santa Cruz Biotechnology, Santa Cruz, CA)]; anti-P-Tyr-STAT1 (Tyr^{701}; ST1P-11A5) mAb (Zymed Laboratories, San Francisco, CA);

Received 10/24/02; accepted 5/30/03.

The costs of publication of this article were defrayed in part by the payment of page charges. This article must therefore be hereby marked *advertisement* in accordance with 18 U.S.C. Section 1734 solely to indicate this fact.

[1] Supported by NIH Grant RO1 AI41769 (to O. M. M.).

[2] To whom requests for reprints should be addressed, at Stanford University School of Medicine, 1201 Welch Road, MSLS P312, Stanford, CA 94305-5492. E-mail: omm@stanford.edu.

[3] The abbreviations used are: LCL, lymphoblastoid cell line; PTLD, posttransplant lymphoproliferative disorder; RAPA, rapamycin; IL, interleukin; STAT, signal transducer and activator of transcription; mTOR, mammalian target of rapamycin; SLCL, spontaneous lymphoblastoid cell line; SCID, severe combined immunodeficient; mAb, monoclonal antibody; P-Tyr, phosphotyrosine; P-Ser, phosphoserine; EMSA, electrophoretic mobility shift assay; CsA, cyclosporine; Jak, Janus-activated kinase.

rabbit antihuman P-Tyr-STAT3 (Tyr^{705}) and rabbit antihuman P-Ser-STAT3 [Ser^{727} (Cell Signaling Technology, Beverly, MA)]; and anti-Jak1 and anti-Tyk2 mAbs (BD Transduction Laboratories, San Diego, CA). RAPA (Rapamune; oral solution) and FK506 (Prograf; i.v. solution) used in the *in vitro* experiments were obtained from the Stanford University Medical Center Pharmacy. RAPA used in the *in vivo* experiments was obtained from Wyeth-Ayerst (Princeton, NJ).

Cell Lines. B LCLs were established by spontaneous outgrowth from the peripheral blood of liver transplant recipients (JB7 and MF4) or lymph node biopsy of a kidney transplant recipient (AB5) with EBV-related PTLD as described previously (12, 14). Briefly, the cell lines were generated by culturing isolated mononuclear cells from the blood or single cell suspensions from the lymph node biopsy in RPMI 1640 (Mediatech, Herndon, VA) with 10% FCS (Hyclone, Logan, UT), 100 μg/ml streptomycin and 100 units/ml penicillin (Life Technologies, Rockville, MD) at 1×10^6 cells/ml in flat-bottomed 96-well plates. After 2 weeks, the surviving cells were expanded and maintained in RPMI 1640 supplemented with 10% FCS (Mediatech) and 100 μg/ml streptomycin and 100 units/ml penicillin. Because the cell lines were established in the absence of growth factors, mitogens, CsA, or exogenous virus, they have been termed SLCLs. The SLCLs are EBV-infected as determined by PCR and Southern blot detection of the viral genome and express the human B-cell markers CD19, CD21, and CD23 (12, 14).

The EBV-infected Daudi Burkitt lymphoma and SKW6.4 B cell lines and the K562 human erythroleukemia cell line were obtained from the American Type Culture Collection (Manassas, VA) and cultured as described above. The JBush LCL was generated by *in vitro* EBV infection of normal human B cells.

***In Vitro* Drug Studies on Cell Growth and Cell Cycle Analysis.** For proliferation experiments, cells were plated in triplicate in a 96-well plate at $1–3 \times 10^5$ cells/ml without or with RAPA (0.1–10 ng/ml) in a final volume of 200 μl/well. Cells were incubated at 37°C for 3 days and pulsed with 0.5 μCi/well [^{3}H]thymidine (New England Nuclear, Boston, MA) for the final 18 h of culture. Total cpm incorporated for triplicate wells were averaged, and data were converted to a percentage of the cpm incorporated by cells grown in media only.

For cell cycle analysis, cells were plated in 24-well plates at 1×10^5 cells/ml in the absence or presence of RAPA (10 ng/ml) and FK506 (30 or 100 ng/ml) in a final volume of 2 ml. After culture for 3 days, cells were washed in PBS and incubated for 30 min in 50 μg/ml propidium iodide, 0.1% Triton X-100, 1 mg/ml sodium citrate, and 1 mg/ml RNase A. Relative DNA content was analyzed on a FACScan flow cytometer using CellQuest software (Becton Dickinson, San Jose, CA).

Mice. Six-week-old, male ICR-scid (SCID) mice were obtained from Taconic Farms (Germantown, NY) and housed in specific pathogen-free conditions in the Stanford Animal Care Facility. Mice were screened for a leaky phenotype by measurement of serum immunoglobulin and excluded from the study if any immunoglobulin was detected.

***In Vivo* Xenogeneic Model for Study of EBV$^+$ B-cell Tumors.** Mice were injected i.p. with 50 μl of rabbit anti-asialo GM_1 antisera (Wako Bio-Products, Richmond, VA) to deplete natural killer cells 1 day before tumor inoculation. On day 0, mice received s.c. injection above the right rear leg with 7.5×10^6 cells of the EBV$^+$ SLCL AB5 or JB7. The RAPA treatment groups of AB5-injected mice ($n = 10$) and JB7-injected mice ($n = 10$) received 1.5 mg/kg/day RAPA i.p. for 8 weeks beginning on the day of tumor injection. The control groups of AB5-injected mice ($n = 8$) and JB7-injected mice ($n = 10$) received daily i.p. injections of the carboxymethylcellulose vehicle.

Tumors were measured in two perpendicular dimensions along the plane of the body every 2–3 days using Vernier calipers. Tumor volume (in mm^3) was calculated using the formula, $0.5ab^2$, where a represents the larger of the two dimensions, and b represents the smaller of the two dimensions.

Histology and Immunohistochemical Staining of Tumor Tissue. Mouse tumor tissue was harvested at the time of sacrifice, fixed in 10% neutral buffered formalin, embedded in paraffin, and sectioned at 0.4-cm intervals. H&E-stained sections were examined concurrently with the patients' original biopsies to confirm the initial diagnoses and to compare the histological features. The lymphoid neoplasms were classified as diffuse large B-cell lymphomas according to the WHO classification system (21).

Serial sections of 4 μm were cut from individual paraffin blocks, deparaffinized in xylene, and hydrated in a graded series of alcohol. Primary antibodies were directed against CD20, Ki-67, and P-Tyr-STAT3. Antigen retrieval by microwave pretreatment was performed in citric acid buffer [10 mM (pH 6.0), 10 min] for CD20 and P-Tyr-STAT3 and in Tris buffer [5 mM (pH 10.0), 20 min] for Ki-67. Endogenous peroxidase was blocked by preincubation with 1% hydrogen peroxide in PBS. Detection of bound primary antibodies was performed using the EnVision + System (DAKO), with a modified biotin-streptavidin technique (DAKO).

Measurement of Human IL-10 in Culture Supernatants and Mouse Sera. SLCLs were plated at 5×10^5 cells/ml in 2 ml of media without or with RAPA (0.1–10 ng/ml). After 2 days, viable cells were counted, and IL-10 in the culture supernatants was quantitated by ELISA as described previously (22), except that capture and detection mAbs were used at 2 and 1 μg/ml, respectively, and 3,3′5,5′-tetramethylbenzidine (TMB) was the substrate used for detection. The amount of IL-10 was normalized to 1×10^6 viable cells for each treatment culture, and the amount of IL-10 produced per million treated cells compared with cells grown in media alone was calculated as a percentage. For *in vivo* studies, mice were bled weekly, and the amount of circulating human IL-10 was determined from serum.

Immunoblots and Immunoprecipitations for Jak/STAT Proteins. Cells cultured in the absence or presence of RAPA (10 ng/ml) for 2–3 days were washed in PBS, and lysates were prepared as described previously (14). Okadaic acid (25 nM) was also included in lysates for P-Ser-STAT3 blots. Equal quantities of protein (10–20 μg) were separated by 7.5% SDS-PAGE under reducing conditions, transferred to nitrocellulose, and probed with the indicated antibodies. Bound antibodies were detected using horseradish peroxidase-labeled secondary antibodies (Jackson Laboratories, West Grove, PA) and enhanced chemiluminescence (Amersham, Piscataway, NJ).

For immunoprecipitations, cells were treated, lysed, and protein quantitated as described previously (14). Equal amounts of protein (1–2 mg) were incubated for 2 h at 4°C with 1 μg of the anti-STAT1α or anti-STAT3 mAb. Twenty μl of GammaBind G-Sepharose (Amersham) were added, and precipitated proteins were electrophoresed and transferred to nitrocellulose. Blots were probed with 1 μg/ml anti-P-Tyr-STAT1, anti-P-Tyr-STAT3, or anti-P-Ser-STAT3 antibodies. Bound antibodies were detected as described above. Subsequently, the same blots were stripped and reprobed using the precipitating antibody. Densitometry was performed on an Alpha Imager 2000 (Alpha Innotech Corp., San Leandro, CA). The ratio of phosphorylated STAT protein to total STAT protein was calculated. For the data in the graphs, the ratios for both the untreated cells and RAPA-treated cells are expressed as a percentage of the ratio determined for the untreated cells.

EMSAs. SLCLs were cultured for 3 days without or with RAPA (10 ng/ml). In some experiments, FK506 (100 ng/ml) was included. Lysates were prepared, and EMSAs were performed as described previously (14) using a ^{32}P-labeled hSIE probe, in the presence or absence of a 100-fold molar excess of unlabeled probe.

Statistical Analysis. Statistical analyses of tumor volume and IL-10 levels were performed using Student's t test, and Ps of <0.05 were considered statistically significant.

RESULTS

RAPA Inhibits Growth of SLCLs *In Vitro*. We have shown previously shown that the calcineurin inhibitor immunosuppressants FK506 and CsA augment the growth of the SLCLs *in vitro* (23). To examine the effects of RAPA on SLCL growth, three PTLD-derived lymphoma lines, AB5, JB7, and MF4, along with Daudi, a Burkitt lymphoma cell line, JBush, an *in vitro* EBV-transformed LCL, and K562, a human erythroleukemia cell line, were cultured with increasing doses of RAPA. Fig. 1*A* shows that proliferation of the SLCLs, as well as Daudi and JBush, is markedly inhibited by RAPA in a dose-dependent manner. In contrast, RAPA has no effect on proliferation of K562.

To determine whether this decrease in proliferation was due to cell growth arrest or apoptosis, cell cycle analysis was performed. RAPA causes an increase in the proportion of spontaneous lymphoblastoid cells in the G_1 phase compared with the proportion of cells in S and G_2/M, indicating an arrest in the G_1 to S transition (Fig. 1*B*). FK506 blocks the ability of RAPA to induce G_1 arrest in the SLCLs in a

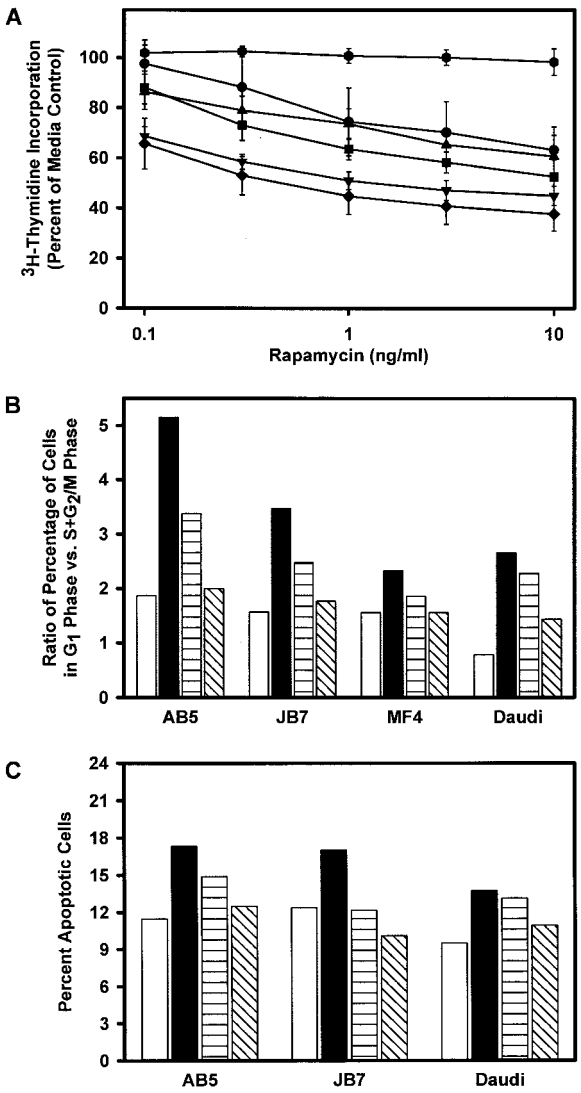

Fig. 1. Inhibition of SLCL growth by RAPA. *A*, cells were incubated with the indicated amount of RAPA for 3 days and pulsed with [^{3}H]thymidine for the final 18 h before harvesting. The cpm incorporated for the RAPA-treated cells were converted to a percentage of the cpm incorporated by cells grown in media only. Mean percentages ± SE from three separate experiments are shown for AB5 (●), MF4 (■), JB7 (▼), Daudi (♦), JBush (▲), and K-562 (*hexagons*). *B* and *C*, cells were incubated in media only (□), 10 ng/ml RAPA (■), 10 ng/ml RAPA + 30 ng/ml FK506 (▤), or 10 ng/ml RAPA + 100 ng/ml FK506 (▧). After 3 days, the percentage of cells in each cell cycle phase was determined by propidium iodide staining and flow cytometry. Data are shown as (*B*) a ratio of the percentage of cells in G_1 *versus* the percentage of cells in S + G_2/M and as (*C*) the percentage of cells with sub-G_1, apoptotic DNA content.

dose-dependent manner. This blocking effect is likely due to competition between RAPA and FK506 for available cellular FK506-binding protein 12, the common intracellular target protein necessary for both drugs to form their active complexes. Simultaneous addition of FK506 also prevents the decrease in proliferation caused by RAPA (data not shown).

To examine the effect of RAPA on apoptosis, the proportion of cells with sub-G_1 DNA content was also determined. RAPA induces a small but reproducible increase in the number of apoptotic cells (Fig. 1*C*). As described above, this effect is also blocked by concurrent addition of FK506. These data indicate that RAPA can inhibit cellular growth of PTLD-associated EBV$^+$ B-cell lines through induction of cell cycle arrest and apoptosis.

Establishment of a Xenogeneic SCID Mouse Model of PTLD. In agreement with previous reports (24, 25), SLCLs form tumors in SCID mice. SCID mice received s.c. injection with 7.5×10^6 cells of the AB5 or JB7 SLCL. Two of two AB5-injected mice and three of four JB7-injected mice developed palpable tumors by 4 weeks postinjection. Animals were sacrificed at 6 weeks, and tumor tissue was harvested for histological and immunohistochemical analysis for comparison with the corresponding patient tumor.

Fig. 2 shows H&E, CD20, and Ki-67 staining of tumors from a representative mouse in each group and an original primary tumor specimen from the same patient that the SLCLs were derived from. Histological features of the tonsils from the patient that the JB7 line was derived from and right axillary lymph node from the patient that the AB5 line was derived from show effacement of normal tonsilar and nodal architecture, respectively. These are replaced by a diffuse sheet-like proliferation of atypical large cells with pleomorphic nuclear outlines, vesicular chromatin, prominent nucleoli, and abundant mitotic activity. These tumors also display foci of necrosis and infiltration into adjacent adipose tissue elements. Immunohistochemistry shows that the tumor cells stain strongly for CD20, confirming their B-cell lineage. In addition, both patient tumors also show an increased growth fraction of 60–80%, as assessed by nuclear staining for Ki-67. The histological and immunophenotypic features of both patient tumors are best classified as diffuse large B-cell lymphomas (monomorphic PTLD) arising in the setting of solid organ transplantation.

The histological features of the tumors established with SLCLs in SCID mice are identical (Fig. 2). The mouse tumors are also comprised of diffuse sheets of large pleomorphic cells with prominent nucleoli infiltrating skeletal muscle and adipose tissue. The tumor cells exhibit abundant mitotic activity and karyorrhexis and are associated with foci of necrosis. Similar to the original patient tumors, the mouse lymphomas show strong staining for human CD20, verifying the human origin of these B-lineage cells, and the Ki-67 stain highlights approximately 60–80% of the tumor cell nuclei. These results indicate that the tumors grown in SCID mice are phenotypically and histologically identical to the primary tumors from patients with PTLD.

RAPA Inhibits SLCL Tumor Growth *In Vivo*. To determine whether RAPA can inhibit tumor growth of SLCLs *in vivo*, SCID mice received injection with 7.5×10^6 AB5 or JB7 cells and were treated for 8 weeks, beginning on the day of tumor inoculation, with either 1.5 mg/kg/day RAPA or carboxymethylcellulose vehicle. Control mice ($n = 10$) injected with JB7 cells developed solid tumors in the second to third week after tumor inoculation (Fig. 3*A*). By 6 weeks postinjection, 10 of 10 animals had visible s.c. tumors, and by 8 weeks, the average tumor volume in the control group was 9376 ± 1785 mm^3 (mean ± SE). In sharp contrast, none of the mice in the experimental group ($n = 10$) had palpable tumors during the 8-week course of RAPA treatment (Fig. 3*C*). One animal subsequently developed a small, visible tumor (94 mm^3) during the ninth week, and a second animal had a small tumor (50 mm^3) at the site of injection that was discovered at autopsy.

Seven of the eight AB5-injected control mice developed solid tumors within 15 days of tumor injection (Fig. 3*B*). By 8 weeks after tumor injection the average tumor volume in the control group was 4421 ± 1277 mm^3. In general, tumors in the AB5 control group were smaller than tumors in the JB7 control group. In contrast to the RAPA-treated JB7 mice, tumors developed in all RAPA-treated AB5 mice (Fig. 3*D*). However, tumor growth in the RAPA-treated AB5 animals was notably delayed, and the average tumor volume of the RAPA-treated group was significantly smaller ($P < 0.05$) than the average tumor volume in the AB5 control group between 2 and 7 weeks postinjection (Table 1). The three mice in the RAPA-treated group with the smallest tumors were removed from treatment 8 weeks after injection (Fig. 3*D*, *inset*). Cessation of RAPA treatment resulted in a dramatic increase in the average tumor volume (from 579 ± 95

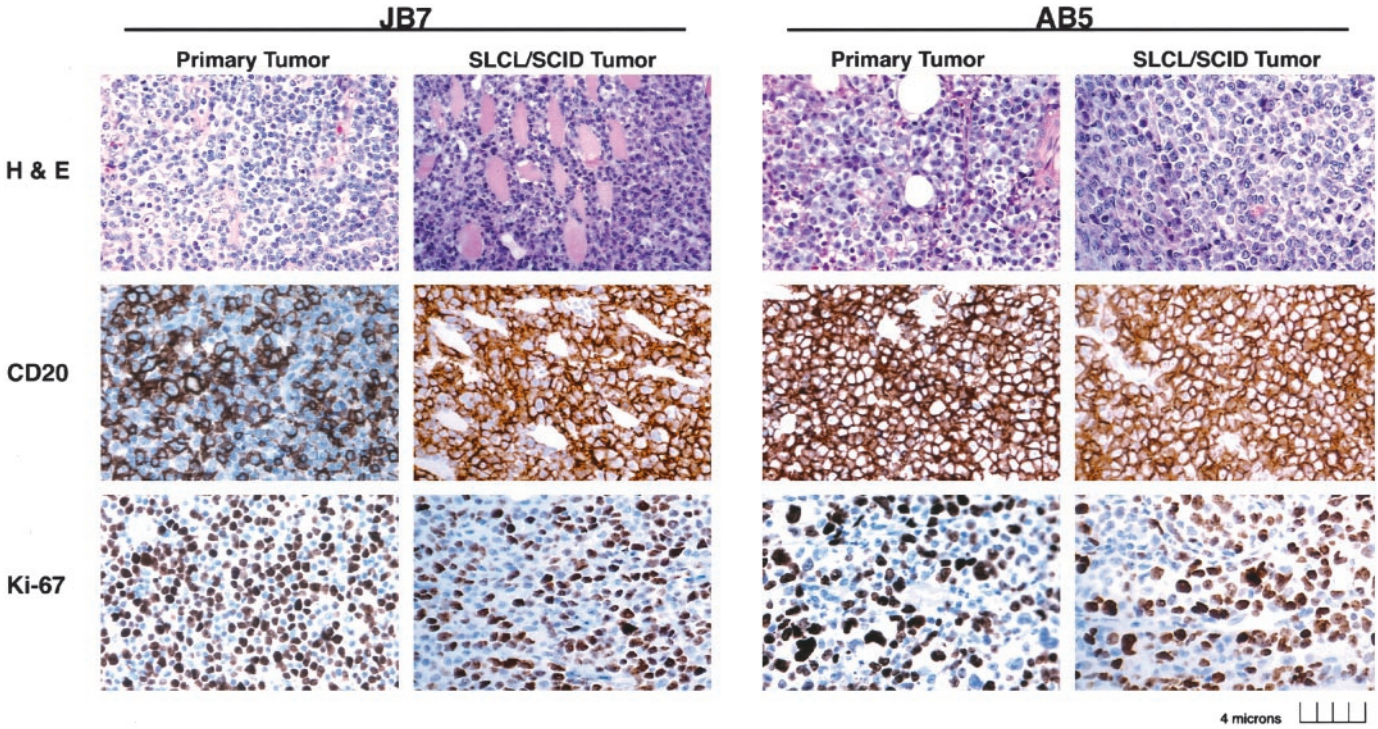

Fig. 2. Primary tumor and SLCL/SCID tumor histology. H&E-, CD20-, and Ki-67-stained paraffin sections of tonsil (JB7 primary tumor) and right axillary lymph node (AB5 primary tumor) with diffuse large cell lymphomas are shown. The H&E, CD20, and Ki-67 stains of representative tumors derived from SCID mice that received injection with JB7 and AB5 SLCL are shown in parallel for comparison. Immunohistochemical stain for CD20 demonstrates strong membrane reactivity compatible with B-cell lineage lymphomas. Immunohistochemical stain for Ki-67 shows nuclear reactivity in 60–80% of the lymphoma cells, indicating a high growth fraction.

mm^3 at 8 weeks to 4555 ± 843 mm^3 at 13 weeks), providing further support that RAPA suppresses tumor growth in these mice. Together, these data indicate that RAPA prevents or slows the growth of solid tumors established from EBV-infected B-cell lines from patients with PTLD.

RAPA Blocks IL-10 Secretion *In Vitro* and *In Vivo*. Our laboratory has demonstrated previously that SLCLs secrete and utilize IL-10 as an autocrine growth factor (12). To determine whether RAPA has an effect on IL-10 production by the SLCLs, ELISAs were performed on supernatants derived from cells cultured without and with RAPA. Daudi cells produce minimal IL-10 (26) and were not included in the experiment. Fig. 4*A* shows that RAPA causes a dose-dependent inhibition of IL-10 production by the SLCLs of over 75% for the three cell lines tested, compared with cells grown in media alone. Note that the cells were counted after drug treatment, and the quantity of IL-10 was normalized to the number of viable cells. The data indicate that the decrease in IL-10 secretion results from a direct effect of RAPA on IL-10 expression and cannot be attributed to fewer cells in the RAPA-treated cultures caused by the antiproliferative effect of the drug. Concurrent addition of FK506 restores IL-10 secretion by the SLCLs (data not shown).

To determine the effect of RAPA on IL-10 secretion *in vivo*, serum levels of human IL-10 were measured in control and RAPA-treated mice. Whereas the average concentration of human IL-10 in the JB7 control group was 125 ± 12 pg/ml at 8 weeks postinjection (Fig. 4*B*), almost no human IL-10 was detected in the sera of the JB7 RAPA-treated group (Fig. 4*D*).

In contrast to the RAPA-treated JB7 mice, RAPA-treated AB5 mice did have detectable levels of IL-10 consistent with tumor growth (Fig. 4*E*). However, at 4 weeks postinjection, the RAPA-treated AB5 group had significantly lower amounts of IL-10 than the control group ($P = 0.002$; Fig. 4, *C* and *E*). By 9 weeks postinjection, the average concentration of circulating human IL-10 in the treated group was 174 ± 51 pg/ml, compared with 1436 ± 511 pg/ml in the control group ($P = 0.01$). This demonstrates a direct correlation between tumor volume and IL-10 levels. For example, the two animals with minimal or no tumor growth in the AB5 control group (Fig. 3*B*) are the same two animals that had minimal or no detectable IL-10 (Fig. 4*C*). In the *in vitro* studies, we could attribute the diminished IL-10 levels in supernatants from RAPA-treated cells to a direct effect of the drug on IL-10 synthesis. However, in the *in vivo* experiments, the reduction in circulating IL-10 most likely reflects the smaller tumor burden in RAPA-treated mice, in addition to a direct effect on the production of IL-10.

STAT3 Is Constitutively Activated in Tumors from Patients with PTLD and in Tumors Established in SCID Mice. Recently, we demonstrated that the SLCLs express constitutively activated proteins of the Jak/STAT signal transduction pathway, likely resulting from autocrine IL-10 stimulation (14). In particular, STAT1 and STAT3 transcription factors remain tyrosine phosphorylated, forming the corresponding DNA-binding homo- and heterodimers. To determine whether constitutive STAT activation is a feature of EBV^+ B-cell lymphomas *in vivo*, we performed immunohistochemical analysis using antibodies to P-Tyr-STAT3 on the original patient tumors and tumors from SCID mice that received injection with JB7 and AB5.

Staining for P-Tyr-STAT3 shows nuclear and cytoplasmic localization within lymphoma cells from both the patients and tumor-bearing SCID mice (Fig. 5). There is no appreciable difference by immunohistochemistry in the number of cells, intensity, or localization of the staining between primary patient tumors and the corresponding lymphomas established in SCID mice. These results indicate that STAT3 is constitutively activated in PTLD lymphomas *in vivo*.

RAPA Decreases Constitutive Jak/STAT Activation in the SLCLs. Because RAPA decreases IL-10 secretion by the SLCLs, and because constitutive STAT activation is associated with PTLD B-cell

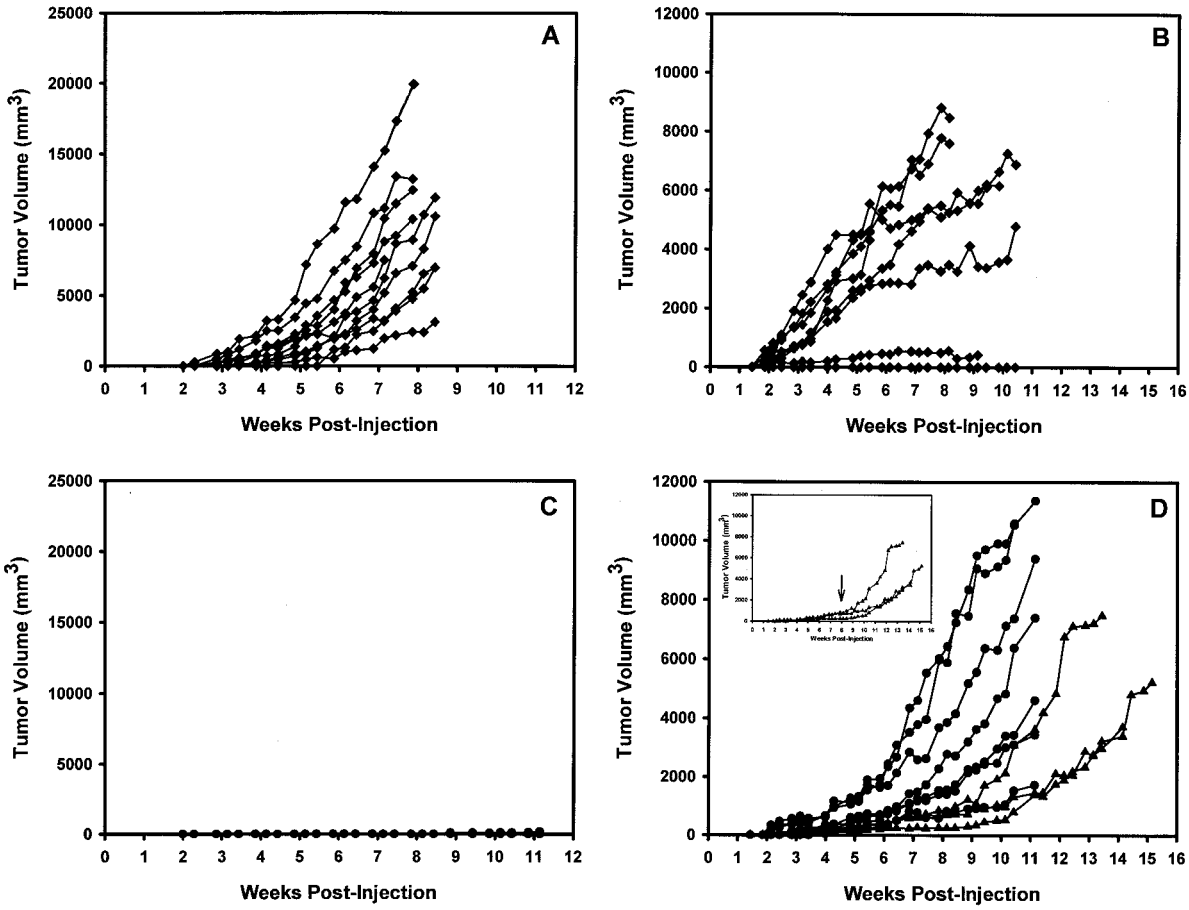

Fig. 3. Effect of RAPA on *in vivo* tumor growth. SCID mice received i.p. injection with 50 μl of anti-asialo GM_1 antisera on day −1. On day 0, mice were injected s.c. with (*A* and *C*) 7.5×10^6 JB7 or (*B* and *D*) 7.5×10^6 AB5 spontaneous lymphoblastoid cells. Beginning on the same day as tumor inoculation, mice received (*A* and *B*) daily i.p. injections of carboxymethylcellulose vehicle or (*C* and *D*) 1.5 mg/kg/day RAPA. Treatment was continued for 8 weeks, and tumor volume was determined every 2–3 days. Control groups, (♦); RAPA-treated groups, (●). *Inset* in *D* shows the increased rate of tumor growth after RAPA treatment was halted (*arrow*) in the three AB5-injected animals with the smallest tumors.

lymphomas, we examined the effect of RAPA on the activation states of STAT1 and STAT3 by EMSA. Fig. 6 (*top panel*) demonstrates that RAPA decreases the quantity of activated STAT1 and STAT3 homo- and heterodimers present in the SLCLs. FK506 reverses this effect, as shown in the JB7 cell line (Fig. 6, *bottom panel*).

The formation of activated STAT dimers is the result of tyrosine phosphorylation and cross-interaction with the SH2 domains. To verify that the decrease in STAT dimers is due to an effect on the activation states of the proteins and not a decrease in the quantity of protein, both STAT1α and STAT3 were precipitated from lysates of untreated and RAPA-treated cells (Fig. 7). Blots were probed with P-Tyr-specific anti-STAT antibodies and then reprobed with the precipitating antibodies. Spot densitometry was performed to compare the amount of phosphorylated protein relative to the amount of total protein. RAPA inhibited tyrosine phosphorylation of STAT1 in the AB5 and JB7 cell lines by 28.8% and 55.1%, respectively, whereas no change was seen in STAT1 tyrosine phosphorylation in the MF4 cell line (Fig. 7*A*). A decrease in STAT3 tyrosine phosphorylation was observed in all SLCLs, with a reduction of 30.4% for AB5, 47.9% for JB7, and 27.2% for MF4 (Fig. 7*B*). The STAT1 tyrosine phosphorylation in the Daudi cell line was also decreased, as was the minimal amount of tyrosine-phosphorylated STAT3 in these cells.

Table 1 *Tumor growth of the AB5 cell line in SCID mice*

Week	Mean tumor volume ± SE (mm^3) RAPA treated (*n*)	Untreated (*n*)	*P*[a]
2	65.2 ± 32.3 (10)	357.8 ± 107.0 (8)	0.012
3	229.1 ± 62.8 (10)	1037.4 ± 292.7 (8)	0.009
4	316.5 ± 70.6 (10)	1926.4 ± 476.1 (8)	0.002
5	636.4 ± 129.8 (10)	2743.1 ± 617.9 (8)	0.002
6	1031.7 ± 239.1 (10)	3302.6 ± 898.4 (7)[b]	0.013
7	1717.2 ± 419.9 (10)	3929.7 ± 1050.9 (7)	0.049
8	2451.8 ± 639.0 (10)	4376.0 ± 1226.1 (7)	0.166

[a] Student's *t* test.
[b] One untreated mouse was sacrificed after week 5.

Depending on the cellular context, serine phosphorylation may also be required for maximal STAT activation (27). In marked contrast to tyrosine phosphorylation, serine phosphorylation of STAT3 in the AB5, JB7, and MF4 cell lines was not affected by RAPA (Fig. 7*C*). Only Daudi cells showed a significant decrease in STAT3 serine phosphorylation (32.7%).

To further verify that the decrease in P-Tyr STAT proteins was not due to a decrease in the expression of proteins involved in the IL-10 signaling pathway, immunoblots were performed. Equal quantities of whole cell lysates from treated and untreated cells were separated and blotted for Jak1, Tyk2, STAT1, and STAT3. As shown in Fig. 7*D*, RAPA does not affect the expression of these proteins.

In summary, these data further support the idea that RAPA not only inhibits cell cycle progression and induces apoptosis but also acts by inhibiting IL-10 production and decreasing the tyrosine phosphorylation of the STAT proteins. This effect is specific to P-Tyr-STAT because RAPA does not inhibit serine phosphorylation of STAT3 or the overall expression of the Jak/STAT proteins in the IL-10 signaling pathway.

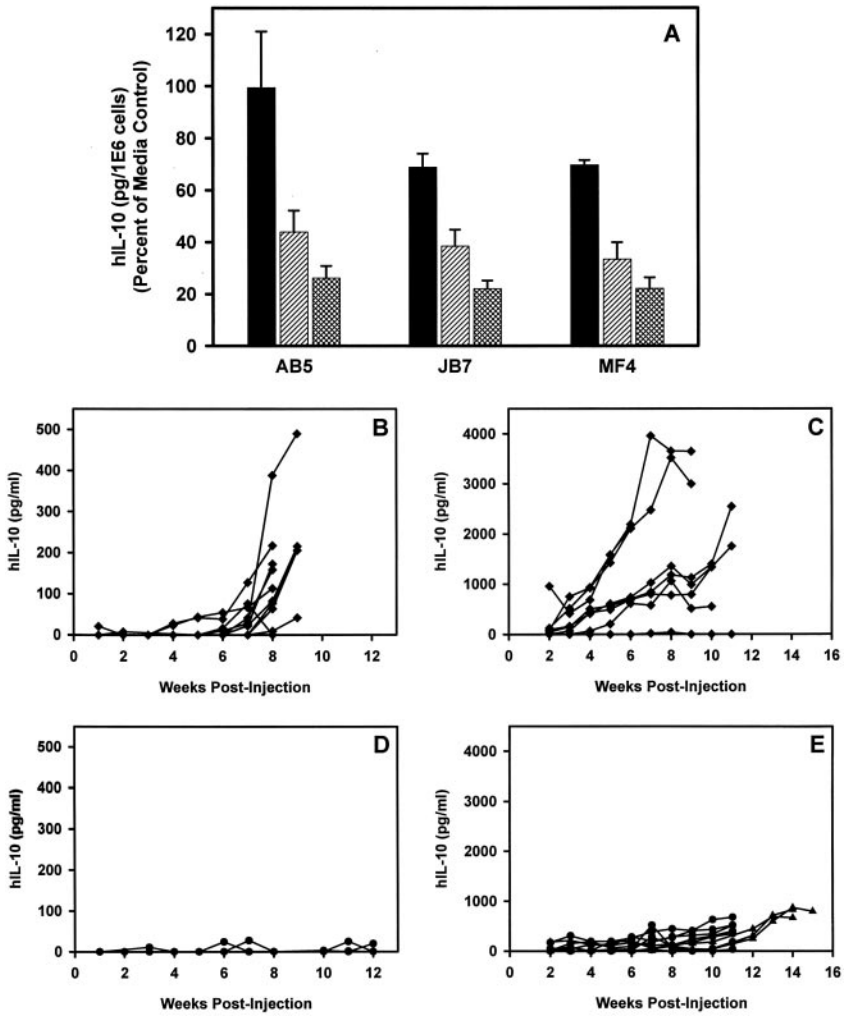

Fig. 4. RAPA inhibits IL-10 secretion by SLCLs *in vitro* and *in vivo*. *A*, SLCLs were cultured without or with 0.1 (■), 1.0 (▨), or 10.0 ng/ml (▩) RAPA. After 2 days, human IL-10 protein levels in the culture supernatants were determined by ELISA and normalized to the number of viable cells in the culture at the time of harvest. Data are expressed as a percentage ± SE of human IL-10 detected per 1×10^6 cells compared with cells grown in media only. Data represent ≥3 experiments/cell line. Serum IL-10 levels were determined weekly in SCID mice injected with (*B* and *D*) 7.5×10^6 JB7 or (*C* and *E*) 7.5×10^6 AB5 spontaneous lymphoblastoid cells. Beginning on the same day as tumor inoculation, mice received (*B* and *C*) daily i.p. injections of carboxymethylcellulose vehicle or (*D* and *E*) 1.5 mg/kg/day RAPA for 8 weeks. Control groups, (♦); RAPA-treated groups, (●); RAPA-treated AB5 mice removed from treatment at 8 weeks, (▲).

DISCUSSION

EBV$^+$ B-cell lymphomas are a serious and potentially fatal complication of solid organ and bone marrow transplantation. The calcineurin inhibitors, CsA and FK506, increase the risk of EBV-related disease because they nonspecifically inhibit T lymphocytes, including EBV-specific CTLs responsible for controlling the expansion of EBV-infected B cells. Treatment options for PTLD are limited, and the prognosis is poor when traditional approaches such as chemotherapy, surgical resection, antiviral medications, or radiation are used (28). The first treatment strategy is usually to reduce or halt immunosuppression to allow the host's immune system to recover and eliminate virally infected cells. However, this approach is often not effective and can precipitate graft rejection.

Here we demonstrate that the immunosuppressive drug RAPA directly inhibits the growth of EBV$^+$ B-cell lymphomas at doses that are therapeutically effective for prevention of graft rejection (18). This observation has significance in the clinical management of transplant patients as well as the prevention and treatment of PTLD. First, these results suggest that the use of RAPA as a component of primary immunosuppression would be prudent in patients at high risk for PTLD, such as graft recipients who are EBV seronegative at the time of transplant. Second, in those patients who develop EBV-related disease while receiving calcineurin inhibitors, it would be preferable to switch to RAPA as primary immunosuppression rather than reducing or halting immunosuppression altogether. RAPA was approved for use in combination with CsA as a prophylaxis for graft rejection in kidney recipients in 1999. Thus, it is a relatively new addition to the array of immunosuppressive drugs used in clinical transplantation, and at present, the effect of RAPA on the development of EBV-related disease is unknown (29).

In this study, we show that RAPA has potent antitumor effects both *in vitro* and *in vivo* on EBV$^+$ B-cell lines derived from patients with PTLD. Moreover, our findings indicate that RAPA targets a mTOR-dependent IL-10 autocrine growth pathway, resulting in diminished IL-10 production and inhibition of constitutive tyrosine phosphorylation of STAT1 and STAT3. Autocrine cytokine pathways are an important mechanism of tumorigenesis and tumor progression in lymphoid malignancies, and disruption of these pathways can have profound effects on tumor growth.

It is plausible that RAPA interferes with the IL-10 autocrine growth axis at multiple sites. Our data clearly demonstrate that RAPA inhibits IL-10 production leading to diminished signaling through the IL-10 receptor. Previous reports have shown that RAPA also inhibits IL-10 production by mitogen-activated T cells (30) and peripheral blood mononuclear cells (31); however, there are no reports showing RAPA inhibition of B-cell derived IL-10 or inhibition of autocrine cytokine pathways.

Our data show that RAPA does not alter the levels of the endogenous Jak/STAT proteins. On the other hand, we cannot rule out the possibility that RAPA also acts downstream of the IL-10 receptor to

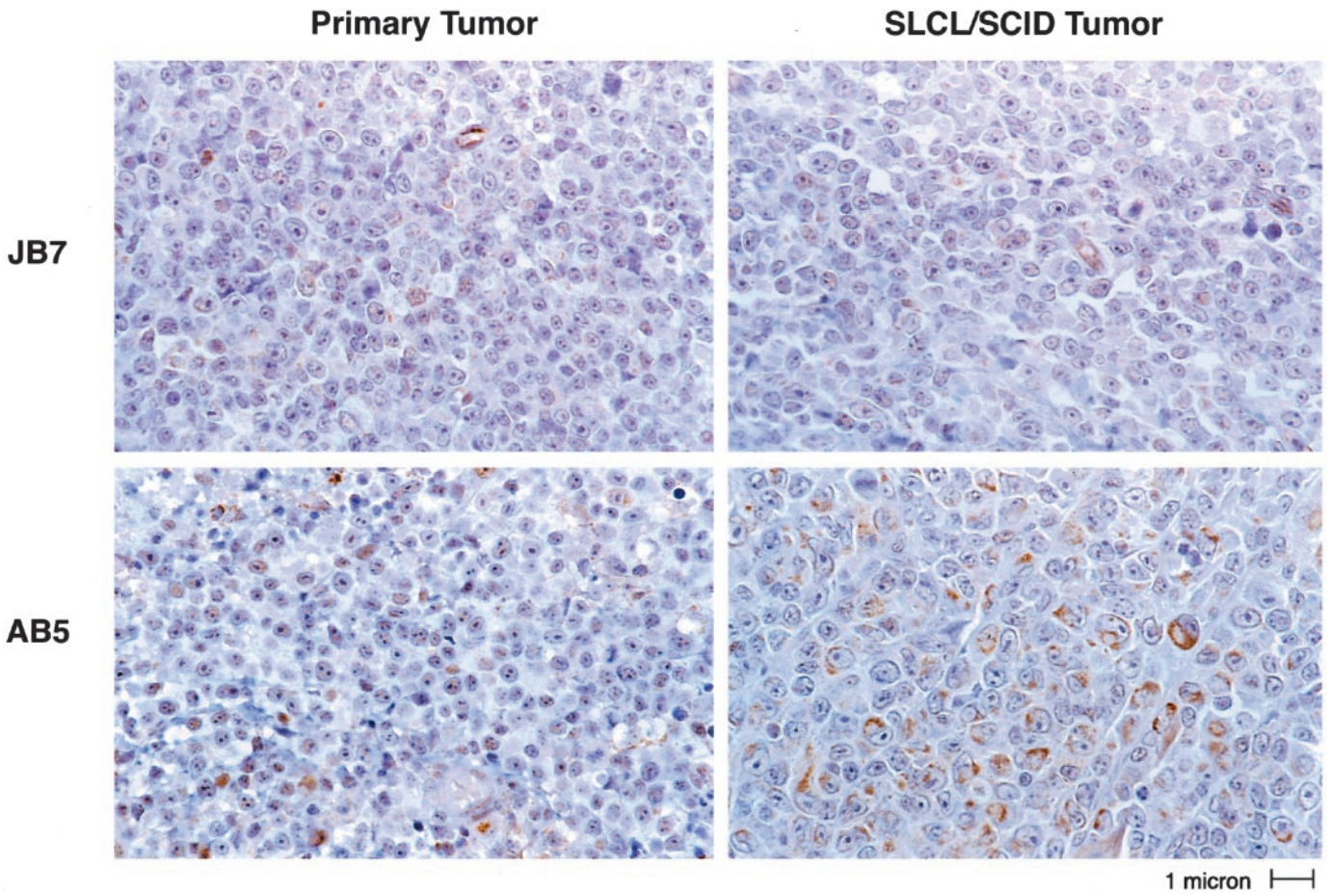

Fig. 5. STAT3 is tyrosine phosphorylated in primary tumors and SLCL/SCID tumors. Immunohistochemical stain for P-Tyr-STAT3 shows nuclear and cytoplasmic staining in the primary patient tumors and in the corresponding tumors derived from SCID mice.

inhibit the constitutive phosphorylation of STAT1 and STAT3, independently of its effect on IL-10 production. Along these lines, it has been shown that tyrosine phosphorylation of STAT3 induced by anti-immunoglobulin in murine B cells is RAPA sensitive and is not due to inhibition of growth factor production (32). Tyrosine phosphorylation of STAT is critical for dimerization, translocation to the nucleus, and binding to STAT-responsive elements. Depending on the stimulus and the cellular context, phosphorylation on Ser^{727} of

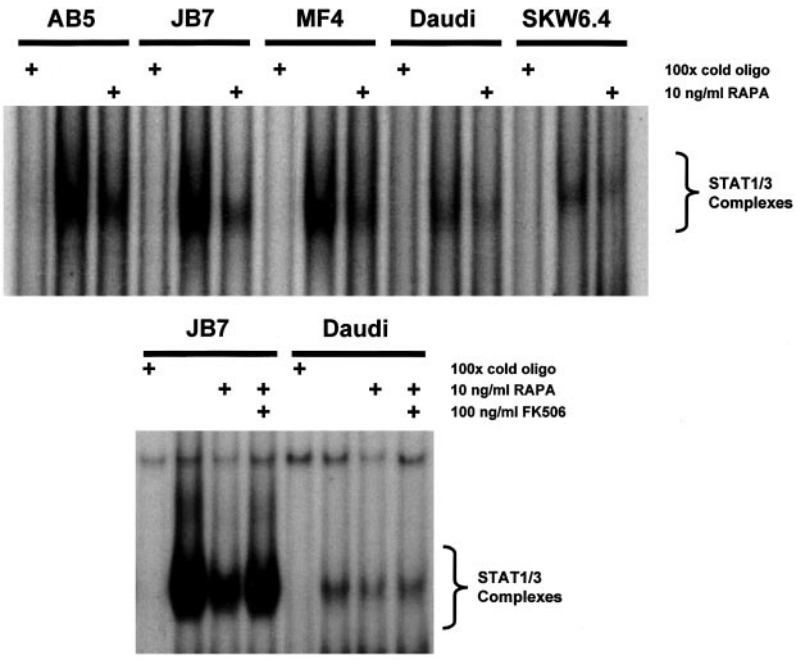

Fig. 6. RAPA inhibits constitutive STAT dimer formation in the SLCLs. Cells were treated for 3 days in the absence or presence of 10 ng/ml RAPA (*top panel*) without and with 100 ng/ml FK506 (*bottom panel*). Extracts were prepared, and 20 μg of protein were incubated with a ^{32}P-labeled hSIE probe, in the presence or absence of a 100-fold molar excess of unlabeled probe (+ *100× cold oligo*). Complexes were separated on a 4% nondenaturing polyacrylamide gel, which was then exposed to film for 18 h at −70°C. Activated STAT1 and STAT3 homo- and heterodimers are indicated.

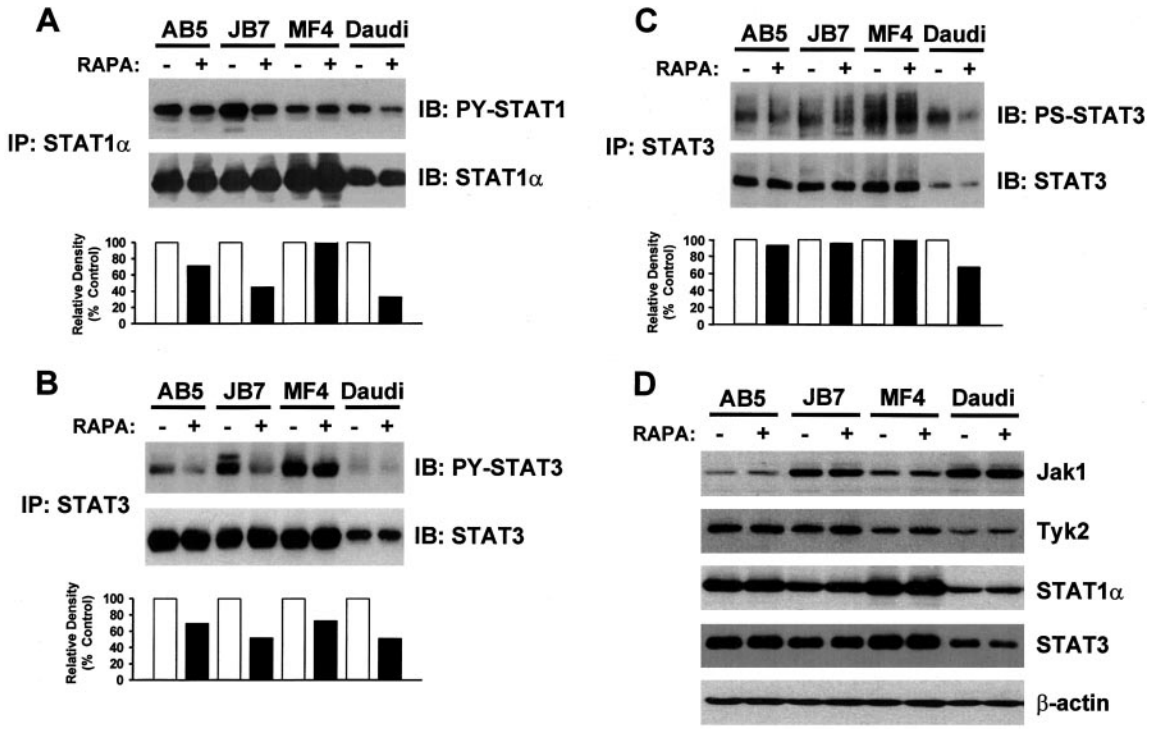

Fig. 7. RAPA inhibits constitutive STAT1 and STAT3 tyrosine phosphorylation but not constitutive STAT3 serine phosphorylation. Cells were untreated (−) or treated (+) for 3 days with 10 ng/ml RAPA, and whole cell lysates were prepared. *A–C*, equal quantities of total protein were immunoprecipitated with the anti-STAT1α (*A*) or anti-STAT3 (*B* and *C*) antibodies indicated on the *left* (*IP*). Immunoblots were probed with P-Tyr- or P-Ser-specific antibodies and then stripped and reprobed with the immunoprecipitating antibodies as indicated on the *right* (*IB*). The ratio of phosphorylated STAT protein to the total STAT protein was determined by densitometry. *Graphs* show the ratios for both the untreated cells (□) and the RAPA-treated cells (■) expressed as a percentage of the ratio determined for the untreated cells for each cell line. One experiment representative of at least three is shown. *D*, equal quantities (10–20 μg) of total protein were separated by 7.5% SDS-PAGE and transferred to nitrocellulose. Blots were probed with antibodies as indicated on the *right*.

STAT3 may also be essential for maximal STAT3 transactivation (27). At least in the case of ciliary neurotrophic factor-stimulated neuroblastoma cells, mTOR can phosphorylate Ser^{727} of STAT3 (33). Although our data indicate that STAT3 Ser^{727} is constitutively phosphorylated in the EBV^+ B-cell lines, RAPA does not effect the serine phosphorylation status of STAT3, suggesting that mTOR does not play a role in serine phosphorylation in these cells.

At present, our data most directly support the idea that RAPA inhibits IL-10-mediated activation of the Jak/STAT signal transduction pathway, resulting in suppression of tumor growth. How activation of the transcription factors STAT1 and STAT3 may drive cellular growth is not known nor are the relevant target genes known. Nevertheless, constitutive STAT activation is a prominent feature of many tumors and has been implicated to have a causal role in tumorigenesis and growth of EBV^+ lymphomas (17, 34). Along these lines, it has been shown that STAT3 is directly oncogenic, causing cellular transformation in rat fibroblasts as well as tumor formation in nude mice (35). Interestingly, tumors that developed in the RAPA-treated AB5 mice showed constitutive STAT3 activation (data not shown). Thus, tumor growth that was not inhibited by RAPA was associated with STAT3 activation.

Other recent studies in experimental animal models also demonstrate the potent antitumor activity of RAPA through unique mechanisms. RAPA showed dramatic antiangiogenic properties that correlated with decreased vascular endothelial growth factor production in a mouse model of metastatic adenocarcinoma (36). In that study, RAPA had minimal direct effect on tumor proliferation but did inhibit metastatic tumor growth *in vivo*. In a mouse model of renal adenocarcinoma, RAPA increased E-cadherin expression, which was associated with conversion from an invasive to a noninvasive phenotype (37). Again, RAPA markedly inhibited tumor progression *in vivo*. Taken together with our findings in a xenogeneic model of PTLD, it appears that the mechanism of RAPA's antitumor effect can vary depending on the tumor type. Thus, RAPA can influence a broad range of biological processes involved in tumor progression including tumorigenesis, growth, survival, and metastasis.

Our *in vitro* experiments showed that RAPA also caused accumulation of cells in the G_1 phase, leading to cell cycle arrest in the G_1 to S transition, and a minor but reproducible induction of apoptosis, both of which were reversed by FK506. Each of these effects by RAPA have been observed in a variety of normal and transformed cells (20). The antitumor activity of RAD, a RAPA derivative, on *in vitro* infected EBV^+ B-cell lines was also attributed to cell cycle arrest and apoptosis (38).

Whereas RAPA was able to suppress tumor growth of the AB5 SLCL, it dramatically inhibited tumor establishment of the JB7 SLCL in a xenogeneic mouse model of PTLD. The reason for the variable sensitivity to RAPA by the two EBV^+ B-cell lymphomas is unknown. However, it is interesting to note that the differences in the effect of RAPA on tumor growth *in vivo* correlate with the relative *in vitro* sensitivities of the two cell lines to RAPA. Accordingly, there was greater inhibition of proliferation, and greater inhibition of STAT1 and STAT3 activation, in the JB7 cell line as compared with the AB5 cell line.

In summary, we report that RAPA inhibits a mTOR-dependent autocrine growth pathway in EBV^+ B-cell lymphomas that is crucial for tumor growth. The data presented here have significant implications for the management of transplant recipients at risk for EBV-related disease because they suggest an approach to simultaneously maintain adequate immunosuppression while deterring the development of EBV^+ B-cell lymphomas. Furthermore, these findings may have significance for the treatment of other EBV-related malignancies.

ACKNOWLEDGMENTS

We are grateful to Dr. Richard Roth for helpful discussion and critical reading of the manuscript.

REFERENCES

1. Young, L. S., Deacon, E. M., Rowe, M., Crocker, J., Herbst, H., Niedobitek, G., Hamilton-Dutoit, S. J., and Pallesen, G. Epstein-Barr virus latent genes in tumour cells of Hodgkin's disease. Lancet, *337:* 1617, 1991.
2. zur Hausen, H., Schulte-Holthausen, H., Klein, G., Henle, W., Henle, G., Clifford, P., and Santesson, L. EBV DNA in biopsies of Burkitt tumours and anaplastic carcinomas of the nasopharynx. Nature (Lond.), *228:* 1056–1058, 1970.
3. Young, L., Alfieri, C., Hennessy, K., Evans, H., O'Hara, C., Anderson, K. C., Ritz, J., Shapiro, R. S., Rickinson, A., Kieff, E., *et al.* Expression of Epstein-Barr virus transformation-associated genes in tissues of patients with EBV lymphoproliferative disease. N. Engl. J. Med., *321:* 1080–1085, 1989.
4. Thorley-Lawson, D. A. Epstein-Barr virus: exploiting the immune system. Nat. Rev. Immunol., *1:* 75–82, 2001.
5. Klein, G. Epstein-Barr virus strategy in normal and neoplastic B cells. Cell, *77:* 791–793, 1994.
6. Busch, L. K., and Bishop, G. A. The EBV transforming protein, latent membrane protein 1, mimics and cooperates with CD40 signaling in B lymphocytes. J. Immunol., *162:* 2555–2561, 1999.
7. Mosialos, G., Birkenbach, M., Yalamanchili, R., VanArsdale, T., Ware, C., and Kieff, E. The Epstein-Barr virus transforming protein LMP1 engages signaling proteins for the tumor necrosis factor receptor family. Cell, *80:* 389–399, 1995.
8. Tosato, G., Tanner, J., Jones, K. D., Revel, M., and Pike, S. E. Identification of interleukin-6 as an autocrine growth factor for Epstein-Barr virus-immortalized B cells. J. Virol., *64:* 3033–3041, 1990.
9. Yokoi, T., Miyawaki, T., Yachie, A., Kato, K., Kasahara, Y., and Taniguchi, N. Epstein-Barr virus-immortalized B cells produce IL-6 as an autocrine growth factor. Immunology, *70:* 100–105, 1990.
10. Durandy, A., Emilie, D., Peuchmaur, M., Forveille, M., Clement, C., Wijdenes, J., and Fischer, A. Role of IL-6 in promoting growth of human EBV-induced B-cell tumors in severe combined immunodeficient mice. J. Immunol., *152:* 5361–5367, 1994.
11. Mauray, S., Fuzzati-Armentero, M. T., Trouillet, P., Ruegg, M., Nicoloso, G., Hart, M., Aarden, L., Schapira, M., and Duchosal, M. A. Epstein-Barr virus-dependent lymphoproliferative disease: critical role of IL-6. Eur. J. Immunol., *30:* 2065–2073, 2000.
12. Beatty, P. R., Krams, S. M., and Martinez, O. M. Involvement of IL-10 in the autonomous growth of EBV-transformed B cell lines. J. Immunol., *158:* 4045–4051, 1997.
13. Masood, R., Zhang, Y., Bond, M. W., Scadden, D. T., Moudgil, T., Law, R. E., Kaplan, M. H., Jung, B., Espina, B. M., and Lunardi-Iskandar, Y. Interleukin-10 is an autocrine growth factor for acquired immunodeficiency syndrome-related B-cell lymphoma. Blood, *85:* 3423–3430, 1995.
14. Nepomuceno, R. R., Snow, A. L., Beatty, P. R., Krams, S. M., and Martinez, O. M. Constitutive activation of Jak/STAT proteins in Epstein-Barr virus B cell lines from patients with posttransplant lymphoproliferative disorder. Transplantation, *74:* 396–402, 2002.
15. Weber-Nordt, R. M., Egen, C., Wehinger, J., Ludwig, W., Gouilleux-Gruart, V., Mertelsmann, R., and Finke, J. Constitutive activation of STAT proteins in primary lymphoid and myeloid leukemia cells and in Epstein-Barr virus (EBV)-related lymphoma cell lines. Blood, *88:* 809–816, 1996.
16. Catlett-Falcone, R., Landowski, T. H., Oshiro, M. M., Turkson, J., Levitzki, A., Savino, R., Ciliberto, G., Moscinski, L., Fernandez-Luna, J. L., Nunez, G., Dalton, W. S., and Jove, R. Constitutive activation of Stat3 signaling confers resistance to apoptosis in human U266 myeloma cells. Immunity., *10:* 105–115, 1999.
17. Garcia, R., and Jove, R. Activation of STAT transcription factors in oncogenic tyrosine kinase signaling. J. Biomed. Sci., *5:* 79–85, 1998.
18. Kahan, B. D., and Camardo, J. S. Rapamycin: clinical results and future opportunities. Transplantation, *72:* 1181–1193, 2001.
19. Hidalgo, M., and Rowinsky, E. K. The rapamycin-sensitive signal transduction pathway as a target for cancer therapy. Oncogene, *19:* 6680–6686, 2000.
20. Sehgal, S. N. Rapamune (RAPA, rapamycin, sirolimus): mechanism of action immunosuppressive effect results from blockade of signal transduction and inhibition of cell cycle progression. Clin. Biochem., *31:* 335–340, 1998.
21. Jaffe, E. S. Tumors of the haematopoietic and lymphoid tissues. *In:* World Health Organization Classification of Tumours. Lyon, France: IARC Press, 2001.
22. Lang, T., Krams, S. M., and Martinez, O. M. Production of IL-4 and IL-10 does not lead to immune quiescence in vascularized human organ grafts. Transplantation, *62:* 776–780, 1996.
23. Beatty, P. R., Krams, S. M., Esquivel, C. O., and Martinez, O. M. Effect of cyclosporine and tacrolimus on the growth of Epstein-Barr virus-transformed B-cell lines. Transplantation, *65:* 1248–1255, 1998.
24. Rowe, M., Young, L. S., Crocker, J., Stokes, H., Henderson, S., and Rickinson, A. B. Epstein-Barr virus (EBV)-associated lymphoproliferative disease in the SCID mouse model: implications for the pathogenesis of EBV-positive lymphomas in man. J. Exp. Med., *173:* 147–158, 1991.
25. Durandy, A., Brousse, N., Rozenberg, F., De Saint Basile, G., Fischer, A. M., and Fischer, A. Control of human B cell tumor growth in severe combined immunodeficiency mice by monoclonal anti-B cell antibodies. J. Clin. Investig., *90:* 945–952, 1992.
26. Burdin, N., Peronne, C., Banchereau, J., and Rousset, F. Epstein-Barr virus transformation induces B lymphocytes to produce human interleukin 10. J. Exp. Med., *177:* 295–304, 1993.
27. Wen, Z., Zhong, Z., and Darnell, J. E., Jr. Maximal activation of transcription by Stat1 and Stat3 requires both tyrosine and serine phosphorylation. Cell, *82:* 241–250, 1995.
28. Paya, C. V., Fung, J. J., Nalesnik, M. A., Kieff, E., Green, M., Gores, G., Habermann, T. M., Wiesner, P. H., Swinnen, J. L., Woodle, E. S., and Bromberg, J. S. Epstein-Barr virus-induced posttransplant lymphoproliferative disorders. ASTS/ASTP EBV-PTLD Task Force and The Mayo Clinic Organized International Consensus Development Meeting. Transplantation, *68:* 1517–1525, 1999.
29. Sindhi, R., Webber, S., Venkataramanan, R., McGhee, W., Phillips, S., Smith, A., Baird, C., Iurlano, K., Mazariegos, G., Cooperstone, B., Holt, D. W., Zeevi, A., Fung, J. J., and Reyes, J. Sirolimus for rescue and primary immunosuppression in transplanted children receiving tacrolimus. Transplantation, *72:* 851–855, 2001.
30. Cohen, S. B., Parry, S. L., Feldmann, M., and Foxwell, B. Autocrine and paracrine regulation of human T cell IL-10 production. J. Immunol., *158:* 5596–5602, 1997.
31. Jorgensen, P. F., Wang, J. E., Almlof, M., Solberg, R., Okkenhaug, C., Scholz, T., Thiemermann, C., Foster, S. J., and Aasen, A. O. Sirolimus interferes with the innate response to bacterial products in human whole blood by attenuation of IL-10 production. Scand. J. Immunol., *53:* 184–191, 2001.
32. Karras, J. G., Wang, Z., Huo, L., Howard, R. G., Frank, D. A., and Rothstein, T. L. Signal transducer and activator of transcription-3 (STAT3) is constitutively activated in normal, self-renewing B-1 cells but only inducibly expressed in conventional B lymphocytes. J. Exp. Med., *185:* 1035–1042, 1997.
33. Yokogami, K., Wakisaka, S., Avruch, J., and Reeves, S. A. Serine phosphorylation and maximal activation of STAT3 during CNTF signaling is mediated by the rapamycin target mTOR. Curr. Biol., *10:* 47–50, 2000.
34. Chen, H., Lee, J. M., Zong, Y., Borowitz, M., Ng, M. H., Ambinder, R. F., and Hayward, S. D. Linkage between STAT regulation and Epstein-Barr virus gene expression in tumors. J. Virol., *75:* 2929–2937, 2001.
35. Bromberg, J. F., Wrzeszczynska, M. H., Devgan, G., Zhao, Y., Pestell, R. G., Albanese, C., and Darnell, J. E., Jr. Stat3 as an oncogene. Cell, *98:* 295–303, 1999.
36. Guba, M., von Breitenbuch, P., Steinbauer, M., Koehl, G., Flegel, S., Hornung, M., Bruns, C. J., Zuelke, C., Farkas, S., Anthuber, M., Jauch, K. W., and Geissler, E. K. Rapamycin inhibits primary and metastatic tumor growth by antiangiogenesis: involvement of vascular endothelial growth factor. Nat. Med., *8:* 128–135, 2002.
37. Luan, F. L., Hojo, M., Maluccio, M., Yamaji, K., and Suthanthiran, M. Rapamycin blocks tumor progression: unlinking immunosuppression from antitumor efficacy. Transplantation, *73:* 1565–1572, 2002.
38. Majewski, M., Korecka, M., Kossev, P., Li, S., Goldman, J., Moore, J., Silberstein, L. E., Nowell, P. C., Schuler, W., Shaw, L. M., and Wasik, M. A. The immunosuppressive macrolide RAD inhibits growth of human Epstein-Barr virus-transformed B lymphocytes *in vitro* and *in vivo*: a potential approach to prevention and treatment of posttransplant lymphoproliferative disorders. Proc. Natl. Acad. Sci. USA, *97:* 4285–4290, 2000.